

A CMOS humidity sensor with on-chip calibration

Y.Y. Qiu^{*}, C. Azeredo-Leme, L.R. Alcácer, J.E. Franca

Center for Microsystems, Instituto Superior Tecnico, Torre Norte 9.09, Avenida Rovisco Pais 1, 1096 Codex Lisboa, Portugal

Accepted 24 November 2000

Abstract

This paper describes a capacitive humidity sensor with on-chip calibration circuit fabricated by a standard CMOS process to achieve a cost-effective solution for accurate and reliable humidity measurement. The humidity sensing property on-chip is obtained by a post-processing step after the standard CMOS fabrication and whereby a commercial polyimide is deposited on the packaged chip. The sensing principle of the sensor is the dielectric constant change of deposited polyimide due to absorption/desorption of water. The on-chip calibration circuit is based on a switched-capacitor front-end, featuring high linearity, insensitivity to temperature, as well as low power consumption. The measured results show that the offset and the sensitivity of the sensor can be precisely calibrated by the integrated circuit which also provides a readable output. The sensor has a linear function with relative humidity in the range of 10–90% RH and a negligible hysteresis. © 2001 Elsevier Science B.V. All rights reserved.

Keywords: CMOS sensor; Humidity sensor; Capacitive sensor; Chemical sensor; Integrated sensor

1. Introduction

As the bulk and surface micromachining techniques [1,2] are getting mature, the integrated silicon sensors fabricated by industrial CMOS IC technologies have received a great interest. A number of microsensors have been fabricated by industrial CMOS technologies without further silicon processing [3–6] or by combining established IC technologies with additional processing steps specific to the sensor function and compatible with the IC process [7–11].

Despite the need of miniaturized, cheap, and reliable humidity sensors in numerous application areas, the humidity microsensors fabricated in standard IC technologies has not yet matured as a commercial product on the market. The classical principles for humidity measurement like psychrometry, dew point, or gravimetric measurement are not applicable for miniaturized sensors, and they are normally expensive and become unstable under continuous use. IC technology allows the integration of the sensor and the circuit on the same chip [11]. This results in a sensor with improvement in sensitivity, linearity, accuracy, interference resistivity, and reduced size. On the other hand, IC is a low cost and batch fabrication technology for manufacturing sensors. However, IC processes limit the range of available

materials and the freedom of the process sequence. Therefore, a few post-processing steps are needed for the fabrication of humidity sensors [8].

The humidity sensing materials, such as dielectric polymers and polyimides, are compatible with IC processes. These materials exhibit fast exchange with water vapor, have low hysteresis, and are chemically stable. However, these materials have poor durability against water and are not applicable at high temperature. To solve this problem, cross-linked polymers has been proposed [12,13].

The objective of the current research is to develop a cheap, accurate, and reliable humidity sensor by integrating the sensing element and the calibration circuitry on a single chip, and using standard CMOS technology for fabrication. The humidity sensing property on-chip is obtained by a simple post-processing step after the standard CMOS fabrication and whereby a commercial polyimide is deposited on the packaged chip.

2. Design and fabrication of the humidity sensor

2.1. Sensing element design

The sensing principle of the humidity sensor presented here is based on the dielectric constant change of deposited polyimide due to absorption/adsorption of water vapor. The sensing element is based on interdigitated capacitance

^{*} Corresponding author. Tel.: +351-21-841-7675;
fax: +351-21-841-7675.
E-mail address: yanyan@gcsi.ist.utl.pt (Y.Y. Qiu).

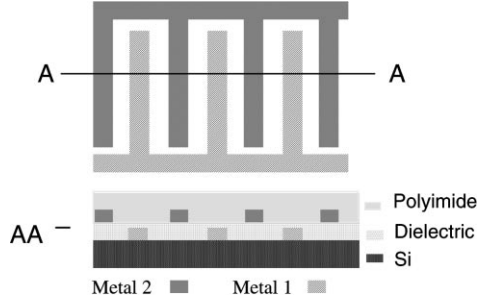


Fig. 1. Schematic structure of sensing element.

structure, as illustrated in Fig. 1. The electrodes are made from two aluminum layers of CMOS technology, metal 1 and metal 2. The size of the entire structure is $308.6 \mu\text{m} \times 308.6 \mu\text{m}$.

2.2. Interface circuit description

Fig. 2 shows the sensor interface circuit. OP2 is an output buffer that can drive an off-chip load. OP1 is a charge-to-voltage converter. In order to compensate the sensor offset and gain errors, dual differential elements are used. One is reference element covered by thick oxide (C_{ref}) and the other is sensing element exposed by adding a passivation-opening layer (C_{sensor}) during CMOS fabrication. Both elements have the same structure, as shown in Fig. 1. The switched-capacitor branch from C_{sensor} to C_1 forms a non-inverting amplifying circuit, and the one from C_{ref} to C_1 forms an inverting amplifying circuit. Feedback capacitor C_2 performs a low-pass function to avoid rapid variation of V_{out} , since humidity is a slow-changing quantity. The dc transfer function of this circuit is

$$V_{\text{out}} = V_{\text{refA}} \left(\frac{C_{\text{sensor}}}{C_1} \right) - V_{\text{refB}} \left(\frac{C_{\text{ref}}}{C_1} \right) \quad (1)$$

where V_{refA} and V_{refB} can be used to adjust the output offset voltage caused by mismatch between C_{sensor} and C_{ref} . The response speed of this circuit is given by a time constant τ

$$\tau = \frac{C_2}{C_1 f_c} \quad (2)$$

where f_c is the clock frequency.

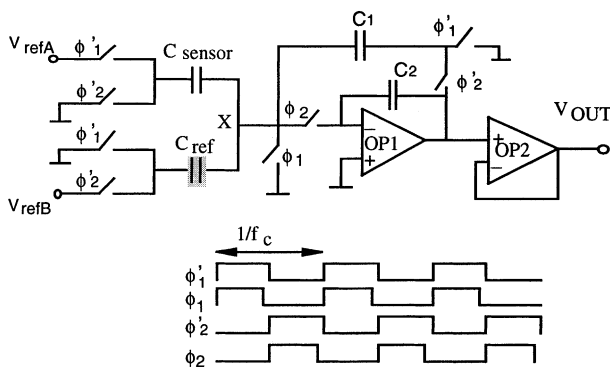


Fig. 2. Sensor interface circuit.

According to transfer function (1), V_{out} has a linear relationship with C_{sensor} . C_{sensor} is a function of the water content of the exposed dielectric. Assuming that the dielectric film covering the sensor has a dielectric constant, ϵ , which varies linearly with relative humidity RH, then ϵ is given by $\epsilon = \epsilon_0 + \alpha\text{RH}$, where α is a constant for an individual sensing material and ϵ_0 the dielectric constant at $\text{RH} = 0$. Therefore,

$$C_{\text{sensor}} = \epsilon K = \epsilon_0 K + K\alpha\text{RH} \quad (3)$$

where K is only depending on the geometry of the sensing capacitor.

Introducing Eq. (3) into Eq. (1), the following equation is formed:

$$V_{\text{out}} = S\text{RH} + b \quad (4)$$

where $S = K\alpha V_{\text{refA}}/C_1$, $b = V_{\text{refA}}(\epsilon_0 K/C_1) - V_{\text{refB}}(C_{\text{ref}}/C_1)$. S represents the sensitivity of the sensor and it is influenced by the value of V_{refA} and the dielectric constant α of the sensing film, and b represents the offset of the sensor and is influenced by both V_{refA} and V_{refB} .

2.3. Interface circuit design considerations

As shown in Fig. 2, the circuit contains three kinds of components: switches, capacitors, and opamps. Sources of the non-linearity of V_{out} versus C_{sensor} include the switches charge injection, non-linear $V-I$ characteristic of capacitors and finite dc gain of opamps. Therefore, to achieve high linearity, metal or poly-poly capacitors are used due to their good $V-I$ linearity. Amplifier OP1 is designed to have very high dc gain (above 100 dB). A two-stage architecture is chosen for both OP1 and OP2. The opamp circuits are shown in Fig. 3 and their electrical characteristics are listed in Table 1.

In switched-capacitor circuits, the clock feed-through and charge injection from switches generates an error voltage in the output. This voltage is related to transistor's threshold voltage and is therefore temperature dependent. To minimize this effect, a four-phase clock scheme shown in Fig. 2 is used [14]. The clock phases ϕ_1 and ϕ_2 drop slightly earlier than ϕ'_1 and ϕ'_2 , respectively, so all switches controlled by ϕ'_1 and ϕ'_2 will not introduce clock feed-through or charge injection errors. Only the two switches connected to the

Table 1
Electrical characteristics of amplifiers

Electrical characteristic	OP1	OP2
dc Gain (dB)	115	120
Gain-bandwidth product (MHz)	9	9
Phase margin (°)	65	70
Supply (V)	3	3
Power consumption (mW)	1.8	5.4

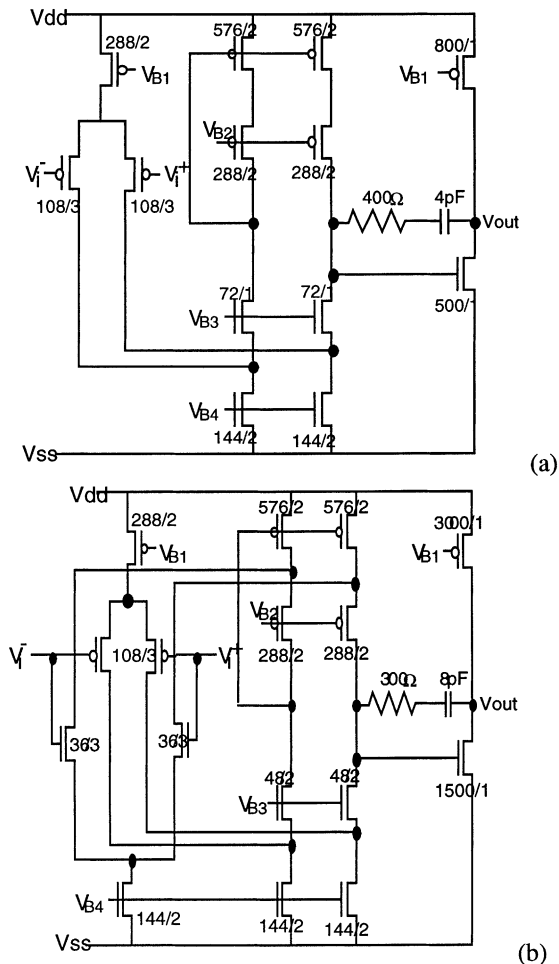


Fig. 3. Opamp circuit: (a) OP1; (b) OP2.

virtual ground of OP1 will affect the output. To minimize this error, the two switches are designed using NMOS devices only and with minimum size. Besides, the capacitor C_1 is designed to have large value.

2.4. Layout of the integrated sensor system and CMOS fabrication

Fig. 4 shows the layout of the sensor system containing a sensing element, a reference element, and on-chip interface circuitry. A pad-opening layer is included to avoid passivation covering of the sensing element during CMOS fabrication. The prototype chips are fabricated in a digital 0.6 μm CMOS process from AMS. The package is a 24-pin DIL (only 12 pins are used).

2.5. Post-processing

After CMOS fabrication, one-step post-processing procedure is necessary to spin-coat a humidity sensitive film on the packaged chip (Fig. 5). Dupont PI2555 is selected as sensing material. The post-processing procedure is described in Table 2.

3. Measurement procedure

Characterization of the sensor is carried out in an AH-202 high/low temperature humidity test chamber. The chamber has a humidity range of 10–98% and temperature range from -40 to $+200^\circ\text{C}$. The humidity and temperature in the chamber can be separately adjusted and kept at constant levels. The deviation of the temperature and humidity during measurement is $\pm 0.25^\circ\text{C}$ and $\pm 3\%$ RH. A commercial heavy duty thermohygrometer is used to obtain the relative humidity and temperature values near the sensor. The thermohygrometer is controlled by a computer through RS-232 communication bus. The output voltage of the sensor is measured with a HP 3458A Multimeter controlled by GP-IB. The saturated salts solutions, such as NH_4Cl , $\text{CaCl}_2 \cdot 6\text{H}_2\text{O}$ and $\text{LiCl} \cdot \text{H}_2\text{O}$ are used for controlling the accuracy of the sensor. At

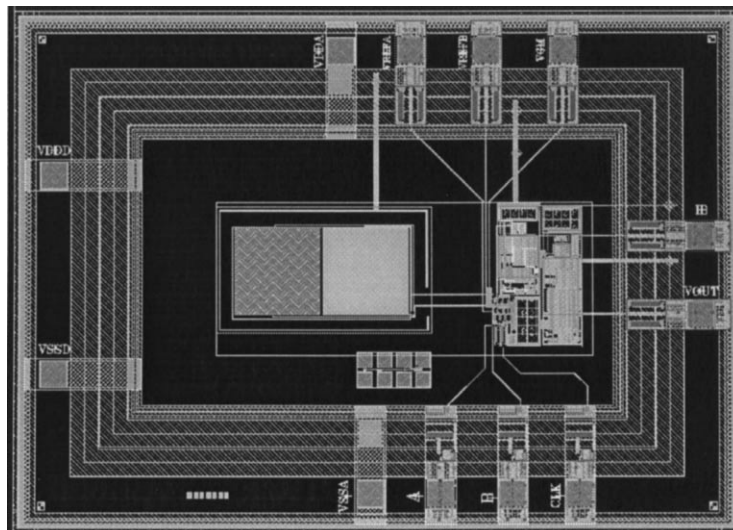


Fig. 4. Layout of the integrated sensor system.

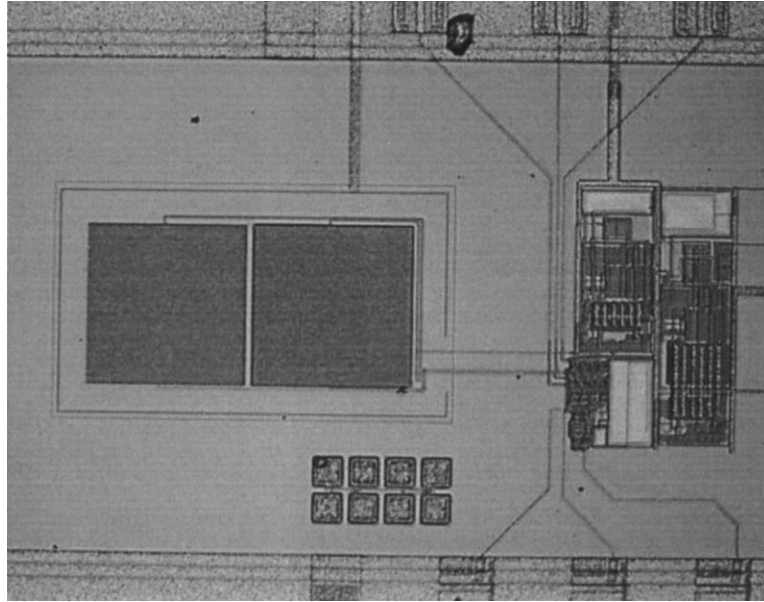


Fig. 5. Photograph of the chip after post-processing with PI2555 and 3.8 μm in thickness.

Table 2
Post-processing procedure of PI2555

Coating	Dispensed PI2555 on the static packaged chip Rotated at 1800 rpm for 5 s Rotated at 2000 rpm for 30 s Finally spin-dried at 1800 rpm for 15 s
Baking	The chip is then baked in convection oven at 120°C for 30 min
Curing	The chip is cured in an oven using the following cure profile Heating from room temperature to 200°C, ramp rate 4°C/min in air Hold at 200°C for 30 min in air Heating from 200 to 330°C, ramp rate 2.5°C/min in nitrogen Hold at 300°C for 60 min in nitrogen Gradual cooling to room temperature
Thickness of the film	3.8 μm

20°C, NH₄Cl, CaCl₂·6H₂O, and LiCl·H₂O saturated solutions provide a constant humidity of 79.5, 32.3, and 15% RH, respectively.

4. Results and discussion

4.1. Sensor sensitivity calibration

The sensor sensitivity (*S*) is defined as the slope of a least squares linear-fit line of *V*_{out} versus RH (%) characteristic. Fig. 6 shows several typical measurements of *V*_{out} versus RH (%) with different input values of *V*_{refA}. *V*_{refB} is adjusted for obtaining a zero value of *V*_{out} at 50% RH. The full range of *V*_{out} is from −1.5 to +1.5 V. The sensing film is 3.8 μm thick PI2555. The ambient RH in the test chamber is programmed between 10–90% RH with steps of 5% RH. All the tests are run at a constant temperature of 26°C. Several measurements are collected per step. Note that the response of the

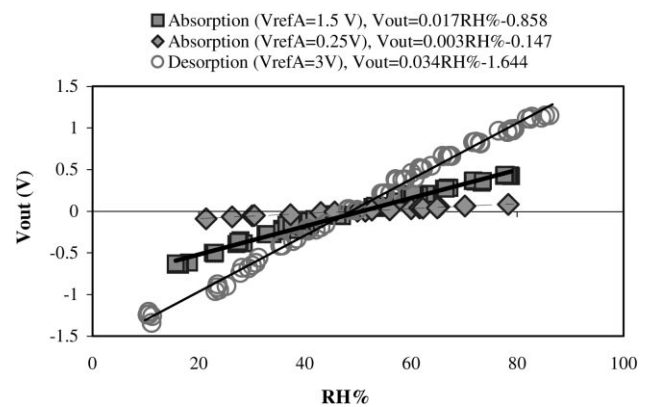
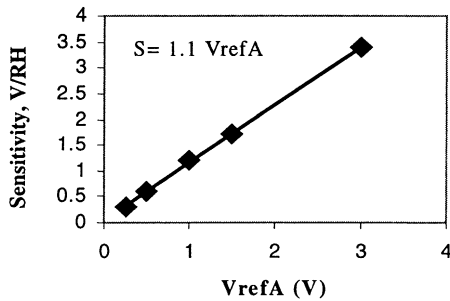


Fig. 6. Sensor *V*_{out} vs. RH with different input values of *V*_{refA} (*V*_{refB} is adjusted for *V*_{out} = 0 at 50% RH). All the tests are running at 26°C.

Fig. 7. Sensitivity as a function of V_{refA} .

sensor is quite linear, with a least squares linear-fit of these data yielding a correlation coefficient greater than 0.99. The sensitivity of the sensor increases as V_{refA} increases, as expected (Eq. (4)). The sensitivity S (in V/RH) as a function of V_{refA} can now be obtained, and it is shown in Fig. 7. The resulting function is

$$S = 1.1V_{\text{refA}} \quad (5)$$

4.2. Sensor offset calibration

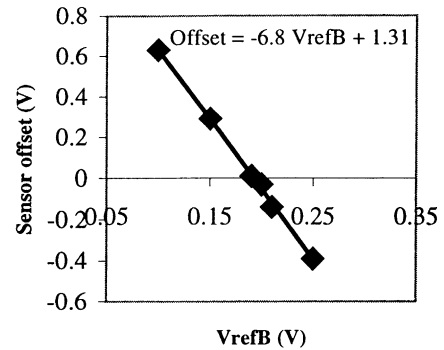
Sensor offset b (in V) is defined as the circuit output for zero RH. Fig. 8 shows that sensor offset is a function of V_{refB} for a constant value of V_{refA} (0.25 V). The resulting characteristic is

$$b = -6.8V_{\text{refB}} + 5.2V_{\text{refA}} \quad (6)$$

Therefore, the transfer function of the sensor for PI2555 sensing film is

$$V_{\text{out}} = (1.1V_{\text{refA}})\text{RH} + (5.2V_{\text{refA}} - 6.8V_{\text{refB}}) \quad (7)$$

The sensor therefore can be calibrated by Eq. (7). Since V_{refA} can be adjusted between 0 and 3 V, the maximum sensitivity of the sensor is 3.3 V/RH. If a maximum V_{refA} is selected, V_{refB} should be correspondingly adjusted in order to avoid the output saturation of the sensor in the measured RH (%) range of 10–100%.

Fig. 8. Sensor offset as a function of V_{refB} with $V_{\text{refA}} = 0.25$ V. All tests are run at 26°C.

4.3. Influence of the dielectric constant of sensing film

According to Eq. (4), sensor transfer function is also influenced by the dielectric constant of the sensing film. In order to prove that, Dupont PI2610 is deposited on the packaged chip with a post-processing procedure described in Table 3. Fig. 9 shows the measurement of V_{out} versus RH (%) for sensors with PI2555 and PI2610 as sensing film, respectively. V_{refA} is adjusted to be 3 V to get the maximum sensitivity to RH changes. Note that the response of the sensors with PI2555 is more sensitive (3.3 V/RH) than with PI2610 (1.6 V/RH). The major difference between PI2555 and PI2610 is their dielectric constant. PI2555 has a larger dielectric constant (3.3 at 1 kHz, 50% RH) than PI2610 (2.9 at 1 kHz, 50% RH). Therefore, the result shown in Fig. 9 indicates that the dielectric constant of the sensing film influences the sensitivity of the sensor as described in Eq. (4).

4.4. Sensor hysteresis

Fig. 10 shows a typical hysteresis measurement. The sensor output voltage is recorded when RH (%) is raised from 20 to 80% (\square , absorption) and then lowered to 20%

Table 3
Post-processing procedure of PI2610

Coating	Dispensed PI2610 on the static packaged chip Rotated at 1800 rpm for 20 s Rotated at 4000 rpm for 20 s Finally spin-dried at 2000 rpm for 20 s
Baking	The chip is then baked in convection oven at 120°C for 30 min
Curing	The chip is cured in an oven using the following cure profile Heating from room temperature to 200°C, ramp rate 4°C/min in air Hold at 200°C for 30 min in air Heating from 200 to 330°C, ramp rate 2.5°C/min in nitrogen Hold at 300°C for 60 min in nitrogen Gradual cooling to room temperature
Thickness of the film	4.2 μm

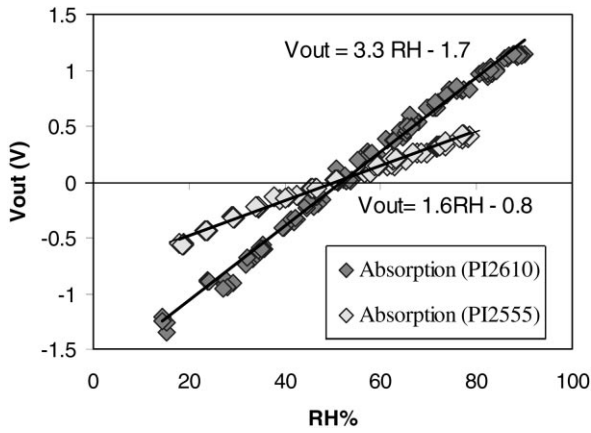


Fig. 9. V_{out} vs. RH (%) for sensing films PI2555 and PI2610; $V_{refA} = 3$ V.

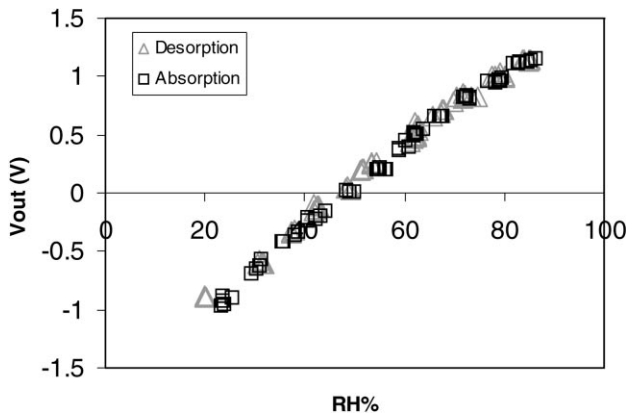


Fig. 10. A typical hysteresis measurement. Sensing film is PI2610; $V_{refA} = 3$ V.

again (Δ , desorption) with a step of 5%. The chamber humidity is corrected by a commercial hygrometer and shown in x -axis. Sensor output voltage is shown in y -axis. No apparent hysteresis is observed. All the data divergence is within the limited resolution of the chamber control.

4.5. Temperature coefficient

An understanding of the temperature dependence of a humidity sensor is critical to the development of an accurate calibration scheme. Fig. 11 shows the continuous record of RH (%) (y_1 -axis) and $T^\circ\text{C}$ (y_2 -axis) versus record time when the test humidity chamber is controlled to maintain a constant RH (%) of $70 \pm 3\%$ (Fig. 11(a)) and $73 \pm 3\%$ (Fig. 11(b)), respectively. When the temperature inside the humidity chamber goes up from 20 to 60°C (see Fig. 11(a)), or goes down from 65 to 30°C (see Fig. 11(b)), the RH (%) measured by the sensor are almost constant except the transient stage due to the chamber control. These phenomena illustrate that the temperature coefficient of the sensor is very small.

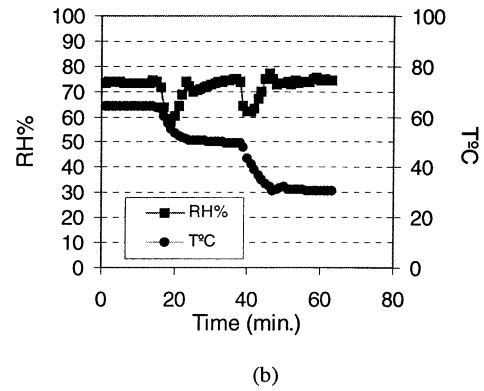
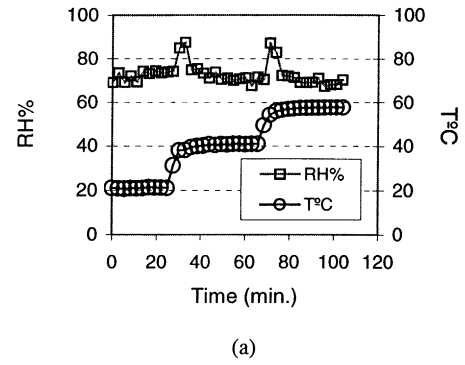


Fig. 11. Typical experimental sequence of RH (%) and $T^\circ\text{C}$ vs. record time with (a) $T^\circ\text{C}$ going up from 20 to 60°C and (b) $T^\circ\text{C}$ going down from 65 to 30°C . The humidity chamber provides a constant RH of $70 \pm 3\%$ ambient.

4.6. Stability

The sensor is aged in a humidity chamber at 60% RH, 26°C for 7 days. The output voltage varies in a range of 0.16–0.24 V corresponding to 57–63% RH due to the limited resolution of the chamber control. But no systematic drift is observable (Fig. 12).

4.7. Response speed

Fig. 13 shows that the RH (%) measured by sensor versus time when changing the humidity rapidly from 79.5 to 10% RH (desorption) and from 15 to 75% RH (absorption).

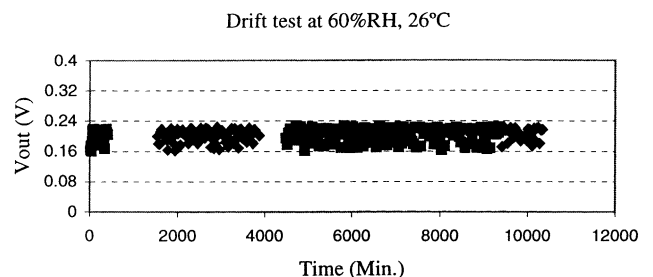


Fig. 12. V_{out} as changes of time in 60% RH at 26°C .

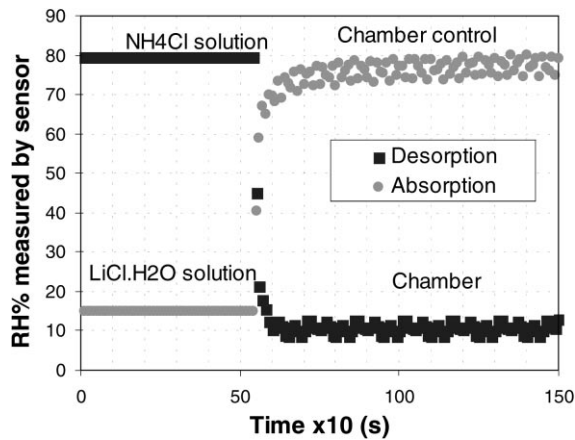


Fig. 13. RH (%) measured by sensor vs. time when changing the humidity from 79.5 to 10% RH, and then from 15 to 75% RH. 79.5 and 15% RH are provided by the saturated salt solution; 10 and 75% RH are obtained by the humidity chamber control.

79.5% RH ambient is provided by NH_4Cl saturated solution and 10% RH ambient is obtained through the humidity chamber control. Similarly, 15% RH ambient is provided by $\text{LiCl}\cdot\text{H}_2\text{O}$ saturated solution, while 75% RH is obtained through chamber control. The result shown in Fig. 13 is obtained in the following way. First, sensor is placed in a small sealed glass container that has an ambient of 79.5% RH (for desorption) and 15% RH (for absorption), respectively. The container is located in the humidity test chamber that has been programmed to have a 20°C and 10% RH ambient for desorption and 75% RH ambient for absorption. When the container reaches the constant RH air, we open the door of the chamber and remove the cover of the container, and the sensor is introduced rapidly into the ambient of the test chamber. Fig. 13 indicates that the response time of the sensor is less than 20 s to reach 80% of the equilibrium value.

4.8. Sensor resolution

The resolution of the sensor is obtained by the following way: (1) measuring sensor output voltage as function of aging time in a constant RH (%) ambient provided by a saturation salt solution NH_4Cl ; (2) translating the sensor output voltages into RH (%) values through the calibrated sensor transfer function (Eq. (7)); (3) plotting the RH (%) values as a function of aging time, as shown in Fig. 14. Note that the RH (%) values varied over a range of 74.94–75% in a constant 75% RH ambient. Therefore, the resolution of the sensor is defined to be 0.06% RH.

4.9. Sensor accuracy after calibration

The sensor accuracy is defined as the sensor error after calibrating for the offset and gain errors. This is dominated then by its non-linearity error. The procedure is as follows.

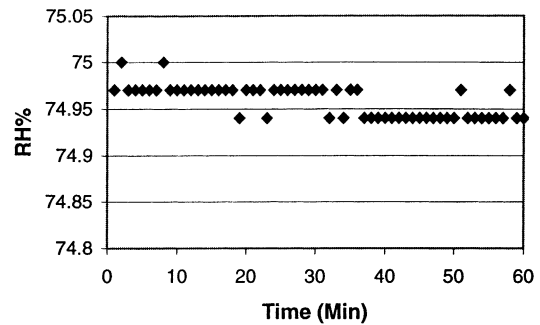


Fig. 14. RH (%) vs. aging time measured in a constant 75% RH ambient.

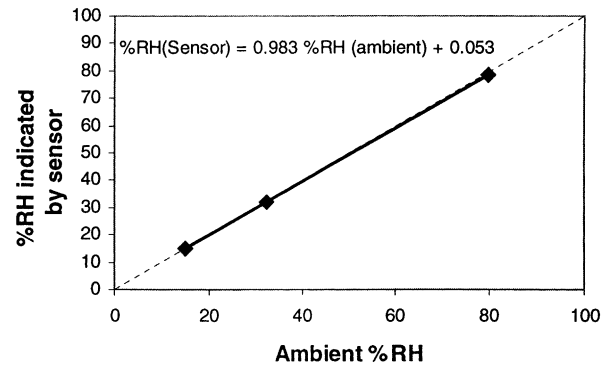


Fig. 15. Sensor accuracy measurement.

1. The sensor is calibrated in the humidity chamber using as many points as possible, as described in Sections 4.1 and 4.2.
2. Using stable reference humidity ambient at 15, 32.2, and 79.5% RH, provided by saturated $\text{LiCl}\cdot\text{H}_2\text{O}$, $\text{CaCl}_2\cdot 6\text{H}_2\text{O}$, and NH_4Cl solutions, respectively, at 20°C, the sensor output voltages were measured and the calibrated RH (%) values were obtained through the calibrated transfer function (Eq. (7)).
3. The calibrated RH (%) as function of the ambient RH (%) is plotted and shown in Fig. 15. The dotted linear line shows an ideal function, i.e.

$$\text{RH} (\%) \text{ measured by sensor} = \text{ambient RH} (\%) \quad (8)$$

The measured data shown as squares represent a linear function of

$$\text{RH} (\%) (\text{sensor}) = 0.983\% \text{RH} (\text{ambient}) + 0.053 \quad (9)$$

The worst deviation of function (9) from (8) during the full RH (%) measurement range (0–100%) is 1.7% RH. This, of course, is the combined effect of all errors in the above procedure, but can be used as a majorant of the sensor accuracy or non-linearity error.

5. Conclusions

An integrated capacitive sensor has been designed and fabricated by CMOS technology combining a simple

additional post-processing step. The humidity sensitive film PI2555 has been successfully deposited on the packaged chip. The on-chip interface circuitry is able to calibrate the sensor offset and the sensitivity precisely. The measured characteristics of the sensor show that the sensor has a linear transfer function and a negligible hysteresis. The resolution of the sensor is 0.06%. No measurable drift is observed after aging the sensor in 60% RH, 26°C for 7 days. The response time of the sensor is about 20 s and the temperature coefficient is very small at high ambient RH.

Acknowledgements

This work is supported by a PEDIP Project, Ecoclimat.

References

- [1] K.E. Petersen, Silicon as a mechanical material, *Proc. IEEE* 70 (1982) 420–457.
- [2] R.T. Howe, Surface micromachining for microsensors and microactuators, *J. Vac. Sci. Technol. B* 6 (1988) 1809–1813.
- [3] H. Baltes, R. Castagnetti, in: S.M. Sze (Ed.), *Semiconductor Sensors: Magnetic Sensors*, Wiley, New York, 1994, pp. 205–269.
- [4] R. Castagnetti, C. Azeredo Leme, H. Baltes, Dual collector magnetotransistors with on-chip bias and signal conditioning circuitry, *Sens. Actuators A* 37/38 (1993) 698–702.
- [5] P. Krummenacher, H. Oguey, Smart temperature sensors in CMOS technology, *Sens. Actuators A* 21–23 (1990) 636–638.
- [6] E.R. Fossum, CMOS image sensors: electronic camera on a chip, technical digest, in: *Proceedings of the IEEE International Electronic Devices Meeting*, Washington, DC, USA, 10–13 December 1995.
- [7] C. Cornila, A. Hierlemann, R. Lenggenhager, P. Malcovati, H. Baltes, G. Noetzel, U. Weimar, W. Goepel, Capacitive sensors in CMOS technology with polymer coating, *Sens. Actuators B* 24/25 (1995) 357–361.
- [8] T. Boltshauser, C. Azeredo Leme, P. O’Leary, H. Baltes, Humidity sensors with on-chip absolute capacitance measurement system, *Sens. Actuators B* 15/16 (1993) 75–80.
- [9] D.T. Jaeggi, C. Azeredo Leme, P. O’Leary, H. Baltes, Improved CMOS Power Sensor, *Transducers 93 Digest of Technical Papers*, IEEE Japan, Tokyo, 1993.
- [10] E. Yoon, K.D. Wise, An integrated mass flow sensor with on-chip CMOS interface circuitry, *IEEE Trans. Electron. Devices* 39 (1992) 1376–1386.
- [11] H. Baltes, Future of IC microtransducers, *Sens. Actuators A* 56 (1996) 179–192.
- [12] M. Matsuguchi, Y. Sadaoka, Y. Sakai, T. Kuroiwa, A. Ito, A capacitive-type humidity sensor using cross-linked poly(methylmethacrylate) thin films, *J. Electrochem. Soc.* 138 (1991) 1862–1865.
- [13] M. Matsuguchi, T. Kuroiwa, T. Miyagishi, S. Suzuki, T. Ogura, Y. Sakai, Stability and reliability of capacitive-type relative humidity sensors using crosslinked polyimide films, *Sens. Actuators B* 52 (1998) 53–57.
- [14] D.G. Haigh, B. Singh, A switching scheme for switched capacitor filters which reduces the effect of parasitic capacitances associated with switch control terminals, in: *Proceedings of the ISCAS’83*, Vol. 2, 1983, pp. 586–589.

Biographies



Y.Y. Qiu graduated with BSc and MSc in Material Science and Engineering from North-east University (PR China), PhD from Institute for Applied Physics, Swiss Federal Institute of Technology (ETHZ), Switzerland. She was researcher in Institute of Corrosion and Protection of Materials of Academia Sinica of PR China from 1987 to 1989 and in Instituto Superior Técnico, Departamento de Materiais, Portugal, from 1994 to 1997. At present, she is a research fellow in Center for Microsystems of

Instituto Superior Técnico (Portugal). Her main research interests relate to solid state sensors, phase relationships and transformations in binary and ternary alloys, microstructural instabilities and high temperature strength superalloys, corrosion and protection of alloys, crystallography analysis.



C. Azeredo-Leme obtained the Engineer degree and MSc in Electronics at Instituto Superior Técnico (IST) in Portugal, and the PhD in Physical Electronics Laboratory in Swiss Federal Institute of Technology (ETHZ), Switzerland. He is currently Assistant Professor in Department of Electrical and Computer Engineering in IST. In 1997, he co-founded CHIPIDEA Microelectronics, the first Portuguese engineering company devoted to the design of advanced mixed-signal integrated circuit products. His main

research interest is in mixed-mode CMOS integrated circuit design, particularly in the area of mobile telecommunications and sensor interfaces.



L.R. Alcácer obtained the PhD degree at the University of California-Riverside in 1970. He was the head of the Instituto Tecnológico e Nuclear in Sacavém until 1975, Assistant Professor at Instituto Superior Técnico (IST) in 1970. In 1975, he obtained the academic degree of “Professor Agregado” and became Full Professor of Chemistry at IST. He is co-founder of IST Centre for Microsystems. His present scientific interests are centered in the area of materials for microsystems including

conducting polymers, polymer electrolytes, sensing materials for chemical, biochemical and humidity sensors, luminescent and semiconducting polymers for electro-optical microsystem elements.



J.E. Franca graduated from Instituto Superior Técnico (IST) (Portugal) in 1978, in 1985 obtained the PhD at Imperial College of Science and Technology (London), and in 1992 obtained the degree of *Agregado* also from IST. He is a Full Professor of the Department of Electrical and Computer Engineering of IST, director and co-founder of IST Centre of Microsystems, President and co-founder of CHIPIDEA Microelectronics, the first Portuguese engineering company devoted to the design of advanced

mixed-signal integrated circuit products. He has actively participated in over 30 R&D projects in the area of mixed analog-digital integrated circuits and systems, particularly in the context of pan-European cooperative efforts involving both Universities and companies. He is currently a member of the Steering Committee of ESSCIRC/ESDERC, a member of the Editorial Board of the *Kluwer Journal on Analog Integrated Circuits and Signal Processing*, and a Fellow of the IEEE, and has been awarded the Golden Jubilee Medal of the Circuits and Systems Society.